

Structure and Nonlinear Optical Properties of Lanthanide Borate Glasses

Kentaro Terashima, Suguru Tamura, Sea-Hoon Kim,[†] and Toshinobu Yoko*

Institute for Chemical Research, Kyoto University, Uji, Kyoto-fu 611, Japan

The third-order nonlinear optical susceptibility, $\chi^{(3)}$, of lanthanide (lanthanum, praseodymium, neodymium, and samarium) borate glasses has been measured by the third harmonic generation method. The structure of the present glass system has been studied by infrared and Raman spectroscopic methods. The network structures of the present $\text{Ln}_2\text{O}_3\text{-B}_2\text{O}_3$ glasses have been confirmed to be basically similar to each other. Praseodymium, neodymium, and samarium borate glasses exhibit $\chi^{(3)}$ values that are larger than lanthanum borate glasses, because of the optical resonance effect, in accordance with the $f\text{-}f$ transition. Especially, the $\chi^{(3)}$ value for $30\text{Pr}_2\text{O}_3\cdot 70\text{B}_2\text{O}_3$ glass is 1.8×10^{-12} esu, which is a factor of ~ 60 larger than that of SiO_2 glass. This striking enhancement of $\chi^{(3)}$ is mainly attributed to the large transition moment to the first excitation state.

I. Introduction

BECAUSE of the development of lasers, the field of nonlinear optics (NLO) has expanded as a new frontier in science and technology. The electric fields that are associated with high-intensity laser beams can be so large that the higher-order nonlinear polarization becomes significant. Among all research criteria of NLO, the development of new materials that possess useful properties is of great importance. Among a variety of materials, glass is considered to be a promising third-order NLO material, because of its optical isotropy and easy fabrication.^{1,2}

In the group of so-called "conventional glasses," B_2O_3 glass is known to be the superior host matrix for the rare-earth metal oxides, because it vitrifies over a wide range of compositions without the addition of any network modifiers. Therefore, lanthanide borate glasses are considered to be proper to investigate the influence of lanthanide ions on the optical properties of these materials.

Thus far, for lanthanide borate glasses, the glass formation region, properties, and structure have been extensively studied.³⁻⁸ Lanthanide ions (Ln^{3+}), in the ground state, have an electronic structure of $[\text{Xe}] 4f^n 5s^2 5p^6$ ($n = 0-14$), where f electrons are shielded by $5s^2 5p^6$ orbitals and, inherently, non-bonding. The number and configuration of $4f$ electrons are known to have a dominant influence on the optical properties. For the lanthanide glasses, the NLO properties are expected to be enhanced, because of the optical resonance effect, which is accompanied by the $f\text{-}f$ electron transition. Therefore, it is in-

teresting to investigate the NLO properties of lanthanide-containing glasses.

In this study, we first examine the structure of the lanthanide borate glasses, based on infrared (IR) and Raman spectroscopic methods for a better understanding of the NLO properties of the glasses. Although the structure of lanthanide borate glasses has already been investigated by Chakraborty and coworkers^{3,4} on the basis of IR spectroscopy, structural investigation on the basis of Raman spectroscopy has not been conducted, except for lanthanum borate glass.³ Then, we estimate the third-order nonlinear optical susceptibility ($\chi^{(3)}$) by the third harmonic generation (THG) method. The variable $\chi^{(3)}$ is discussed in terms of the optical resonance effect, which is related to the $f\text{-}f$ electron transition.

II. Experimental Procedure

Reagent-grade La_2O_3 , Pr_6O_{11} , Nd_2O_3 , and Sm_2O_3 (Wako Pure Chemical Industries, Osaka, Japan) and reagent-grade B_2O_3 (Nacalai Tesque, Kyoto, Japan) were used as raw materials. The batch composition of $\text{Ln}_2\text{O}_3\text{-B}_2\text{O}_3$ ($\text{Ln} = \text{La, Pr, Nd, and Sm}$) binary glasses are shown in Table I. A 10 g batch of well-mixed reagents was melted in a Pt-10%-Rh crucible that was covered with a lid at 1400°C - 1500°C for 10 min in an electric furnace. The glasses were obtained by pouring the melts onto a stainless-steel plate and by pressing them with another stainless-steel plate. The glasses were polished to ~ 1 mm thick for the measurements of the various optical properties.

The reference metaborate crystal, LaB_3O_6 , was prepared by heating $25\text{La}_2\text{O}_3\cdot 75\text{B}_2\text{O}_3$ glass at 850°C for 12 h. The devitrified material was identified to be LaB_3O_6 crystal via X-ray diffractometry (XRD) analysis.

IR spectra were measured via KBr pellet techniques with a Fourier transform infrared spectroscopy (FTIR) spectrophotometer (Model FTIR-8000 Series, Shimadzu Co., Kyoto, Japan) in the frequency range of $400\text{-}2000\text{ cm}^{-1}$. Raman spectra of the glasses were measured with a Raman spectrophotometer (Model JASCO NR-1000S, Nippon Bunko, Tokyo, Japan), using the 488.0 nm lines (neodymium borate glasses) as well as the 514.5 nm lines (lanthanum, praseodymium, and samarium borate glasses) of an argon-ion laser as the excitation beam, to avoid fluorescence from the excited state. The power was adjusted to 250-300 mW. The light that was scattered at an angle of 90° and passed through a double-grating monochromator was detected by a photomultiplier, and then the signal was stored and processed in a computer. The resolution and the precision of the wavenumber were within 1 cm^{-1} . The measured Raman spectra were corrected for thermal population.

The THG values of the glasses were measured via a NLO measurement apparatus (Tokyo Instruments, Tokyo, Japan). A Q-switched neodymium-doped yttrium aluminum garnet (YAG) laser was operated at the fundamental wavelength of $1.064\text{ }\mu\text{m}$ with a pump pulse duration of 10 ns and maximum power density of 200 MW/cm^2 . The laser frequency at $1.9\text{ }\mu\text{m}$ was obtained directly by stimulated Raman scattering in a high-pressure hydrogen cell that was excited by the $1.064\text{ }\mu\text{m}$ Nd line. To avoid damage to the glasses, the $1.9\text{ }\mu\text{m}$ beam was

G. H. Sigel Jr.—contributing editor

Manuscript No. 191910. Received September 9, 1996; approved April 6, 1997. Supported by a Grant-in-Aid for Scientific Research from the Ministry of Education, Science and Culture of Japan. Author TY would like to acknowledge the partial support of The Iketani Science and Technology Foundation.

*Member, American Ceramic Society.

[†]Present address: Ceramic Materials Research Institute, Hanyang University, Seoul 133-791, Korea.

Table I. Linear and Nonlinear Optical Properties[†] of Lanthanide Borate Glasses

Composition (mol%)	Density (g/cm ³)	T_{ω} (%)	$T_{3\omega}$ (%)	n_{ω}	$n_{3\omega}$	E_g (eV)	l_c (μ m)	I/I_{SiO_2}	$\chi^{(3)}$ ($\times 10^{-14}$ esu)
20La ₂ O ₃ ·80B ₂ O ₃	3.918	92.7	81.8	1.645	1.673	6.39	12.6	1.15	5.94
25La ₂ O ₃ ·75B ₂ O ₃	3.941	90.4	81.2	1.657	1.678	6.01	12.0	1.29	6.82
30La ₂ O ₃ ·70B ₂ O ₃	4.187	88.4	79.0	1.701	1.721	5.76	10.9	2.08	10.3
20Pr ₂ O ₃ ·80B ₂ O ₃	4.122	0.8	81.4	1.671	1.690	4.78	12.2	0.53	151
25Pr ₂ O ₃ ·75B ₂ O ₃	4.216	0.4	80.9	1.672	1.698	4.76	11.6	0.21	169
30Pr ₂ O ₃ ·70B ₂ O ₃	4.526	0.2	68.1	1.723	1.777	4.71	10.6	0.06	186
20Nd ₂ O ₃ ·80B ₂ O ₃	4.255	88.4	68.1	1.698	1.724	5.68	12.7	1.24	7.06
25Nd ₂ O ₃ ·75B ₂ O ₃	4.566	87.3	66.1	1.703	1.731	5.65	11.3	1.59	9.20
30Nd ₂ O ₃ ·70B ₂ O ₃	4.633	85.7	63.8	1.754	1.777	5.61	9.98	2.71	14.7
20Sm ₂ O ₃ ·80B ₂ O ₃	4.685	45.9	83.4	1.689	1.715	4.86	13.0	1.50	11.7
25Sm ₂ O ₃ ·75B ₂ O ₃	4.693	44.3	82.6	1.695	1.719	4.84	11.8	1.22	12.0
30Sm ₂ O ₃ ·70B ₂ O ₃	4.767	37.2	78.2	1.697	1.720	4.80	10.2	1.03	14.8

[†] T_{ω} and $T_{3\omega}$ are the apparent transmittances at 633 nm and 1.9 μ m, respectively; n_{ω} and $n_{3\omega}$ are the refractive indices at 633 nm and 1.9 μ m, respectively; E_g is the optical band gap; l_c is the coherence length; I/I_{SiO_2} is the relative intensity of the third harmonic signal; and $\chi^{(3)}$ is the third-order nonlinear optical susceptibility.

appropriately attenuated via Nd filters. After being isolated by a monochromator, the third harmonic wave at 633 nm was detected by a photomultiplier at the gate width of 30 ns. The sample was mounted on a goniometer and rotated at angles from +45° to -45° by a computer-controlled stepping motor, with respect to the axis that is perpendicular to the 1.9 μ m incident beam. The methods to measure the optical absorption spectra and the refractive index have been described in detail elsewhere.^{9,10}

III. Results

(1) Density, Refractive Index, and IR and Raman Spectra

The density, transmittance (T), refractive index (n), and optical band gap (E_g) values are listed in Table I. The subscripts ω and 3ω correspond to the wavelengths 1.9 μ m and 633 nm, respectively. The n value at 1.9 μ m was obtained from the extrapolation of $1/(n^2 - 1)$ -vs- E^2 plots (E is the photon energy) roughly by assuming Wemple's single-oscillator model.¹¹ Figure 1 shows the absorption spectra of 30Ln₂O₃·70B₂O₃ (Ln = La, Pr, Nd, and Sm) glasses. The colors of the glasses are colorless, light green, purple, and yellow for the lanthanum, praseodymium, neodymium, and samarium borate glasses, respectively. In Table I, the E_g values of these glasses are also given. E_g was estimated from the extrapolation of the $(AE)^2$ -vs- E linear plot to the E -axis, as shown in Fig. 2, where A is the absorption coefficient and E is the photon energy (equal to $h\nu$).

Figure 3 shows the IR spectra of 30Ln₂O₃·70B₂O₃ (Ln = La, Pr, Nd, and Sm) binary glasses. The IR spectra exhibit three broad absorption bands at 1400, 1000, and 680 cm⁻¹, which are assigned to the stretching modes of BO₃ and BO₄ units and to the B–O–B bending mode, respectively.¹² As the atomic number of the lanthanide ion increases, all these absorption bands shift to low wavenumbers, which is caused by the increase of the field strength of the Ln³⁺ ion.

Figures 4 and 5 show the Raman spectra of the La₂O₃–B₂O₃ system and 30Ln₂O₃·70B₂O₃ (Ln = La, Pr, Nd, and Sm) glasses, respectively. The band assignment of Raman spectra is summarized in Table II.^{8,13} A band characteristic of the boroxol group, which appears at 808 cm⁻¹ in the low-rare-earth-content glass,⁴ was not observed in the glasses that contained >20 mol% La₂O₃. As the atomic number of the lanthanide ion increased, the Ln–O stretching modes shifted to high wavenumbers. This mode shift was also ascribed to the increase of the field strength of the Ln³⁺ ion.

(2) Linear and Nonlinear Optical Properties

E_g of lanthanide borate glasses is shown as a function of Ln₂O₃ content in Fig. 6. We notice from Fig. 6 that, except for lanthanum borate glasses, the E_g value abruptly decreases from 7.2 eV for B₂O₃ glass to 4.78, 5.68, and 4.86 eV for praseodymium, neodymium, and samarium borate glasses, respectively, by the addition of 20 mol% of Ln₂O₃ and then gradually decreases as the Ln₂O₃ content is increased further. For lanthanum borate glasses, E_g decreases almost linearly as the

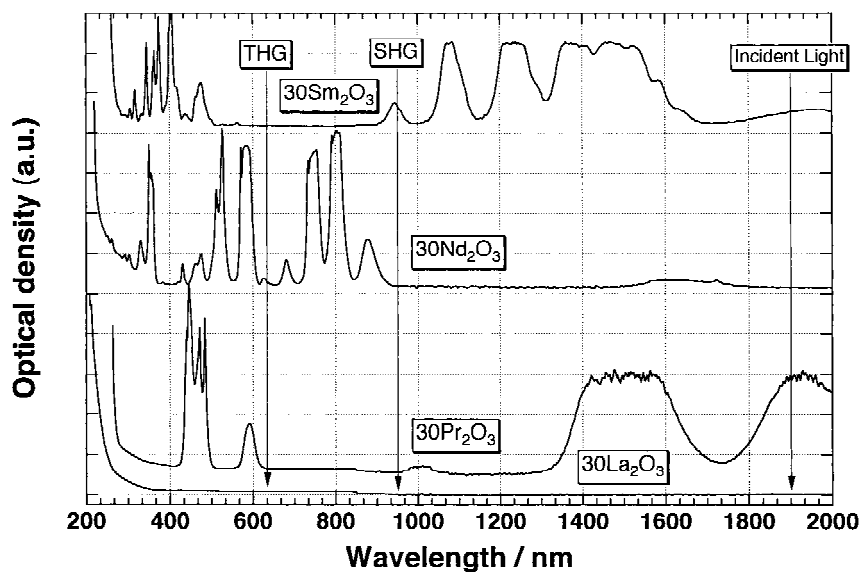


Fig. 1. Absorption spectra for 30Ln₂O₃·70B₂O₃ (Ln = La, Pr, Nd, and Sm) binary glasses.

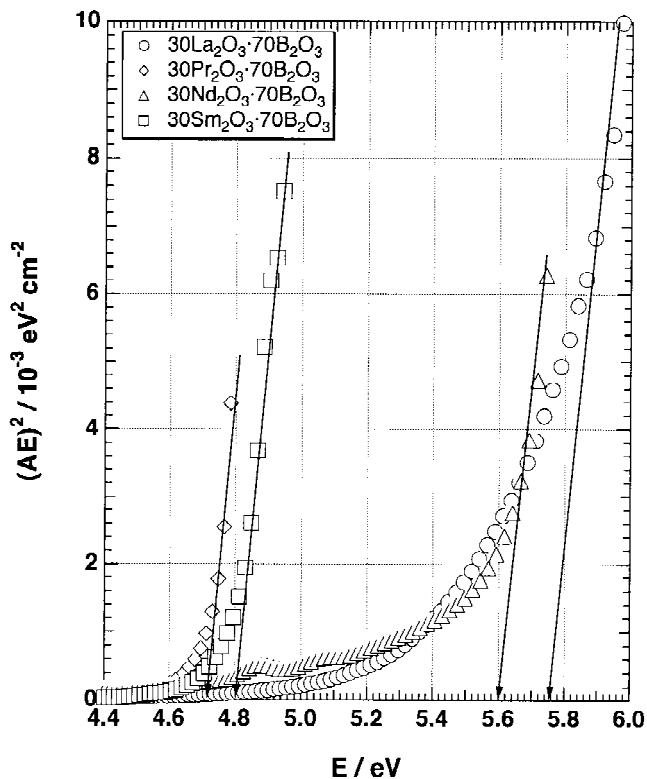


Fig. 2. Variation of $(AE)^2$ with E in $30\text{Ln}_2\text{O}_3\cdot 70\text{B}_2\text{O}_3$ ($\text{Ln} = \text{La}, \text{Pr}, \text{Nd}, \text{and Sm}$) binary glasses; the optical band gap, E_g , was estimated from the extrapolation of the $(AE)^2$ -vs- E linear plot to the E -axis.

La_2O_3 content increases. These results suggest that microscopic aggregation of Ln^{3+} ions may occur in praseodymium, neodymium, and samarium borate glasses.

Figure 7 shows the third harmonic signal as a function of the incident angle for $30\text{La}_2\text{O}_3\cdot 70\text{B}_2\text{O}_3$ glass. The THG intensity pattern of SiO_2 glass also is shown in this figure as a reference. To eliminate the contribution from the upconversion luminescence, the intensity of the third harmonic signal has been obtained from the difference between the upper and lower envelopes of the fringe pattern.

The coherence length, l_c , of the sample was obtained from the fringe patterns as follows:⁹

$$l_c = \frac{d}{2(j-i)} \left[\frac{1}{(1 - \sin^2 \theta_j / n_\omega^2)^{1/2}} - \frac{1}{(1 - \sin^2 \theta_i / n_\omega^2)^{1/2}} \right] \quad (1)$$

where d is the sample thickness, i and j are the fringe numbers, and θ_i and θ_j are the incident angle of the i -th and j -th fringes, respectively.

The third-order nonlinear optical susceptibility, $\chi^{(3)}$, was calculated by using the following expression:^{9,10}

$$\chi^{(3)} = \chi_{\text{SiO}_2}^{(3)} \left(\frac{l_{c,\text{SiO}_2}}{l_c} \right) \left(\frac{I}{I_{\text{SiO}_2}} \right)^{1/2} \left(\frac{n_{3\omega} n_\omega^3}{n_{3\omega,\text{SiO}_2} n_{\omega,\text{SiO}_2}^3} \right)^{1/2} \times \left(\frac{T_{3\omega,\text{SiO}_2}^{1/2} T_{\omega,\text{SiO}_2}^{3/2}}{T_{3\omega}^{1/2} T_\omega^{3/2}} \right)^{1/2} \quad (2)$$

The subscript SiO_2 denotes silica glass. I/I_{SiO_2} is the relative intensity of the third harmonic signal, with respect to SiO_2 glass. The values of transmittance T and refractive index n of silica glass are as follows: $T_{3\omega,\text{SiO}_2} = 93.5\%$, $T_{\omega,\text{SiO}_2} = 94.7\%$, $n_{3\omega,\text{SiO}_2} = 1.457$, and $n_{\omega,\text{SiO}_2} = 1.439$. The values of $\chi_{\text{SiO}_2}^{(3)} = 2.8 \times 10^{-14}$ esu and $l_{c,\text{SiO}_2} = 18.1 \mu\text{m}$ were used for the calculation of $\chi^{(3)}$.

The $\chi^{(3)}$ values of lanthanide borate glasses are plotted as a

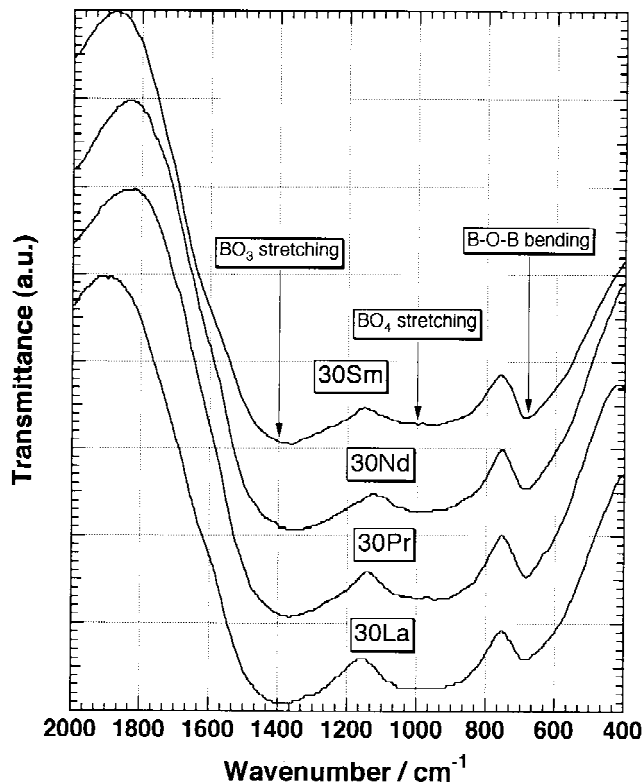


Fig. 3. IR spectra of $30\text{Ln}_2\text{O}_3\cdot 70\text{B}_2\text{O}_3$ ($\text{Ln} = \text{La}, \text{Pr}, \text{Nd}, \text{and Sm}$) binary glasses.

function of Ln_2O_3 content in Fig. 8. As shown in this figure, they increase as the Ln_2O_3 content increases in each glass system and, at any composition, increase in the following order of lanthanide element: $\text{La} < \text{Nd} < \text{Sm} \ll \text{Pr}$.

IV. Discussion

(1) Structure of Lanthanide Borate Glasses

For lanthanide borate glasses, on the basis of the IR spectra, Chakraborty *et al.*⁴ concluded that the glass structure near the metaborate composition consisted of borate networks, similar to their crystalline counterpart. The schematic structure model of the lanthanide metaborate (LnB_3O_6) crystal is shown in Fig. 9.¹⁴ The ladder-type chains are composed of BO_3 trigonal and BO_4 tetrahedral units in a 2:1 ratio and are interconnected by lanthanide ions that are coordinated by approximately ten oxygen atoms.¹⁴ The stability of lanthanide metaborates is primarily determined by the O-O separation between adjacent $(\text{B}_3\text{O}_6)_z$ chains. It is reported that the europium, gadolinium, and holmium borate systems, each of which have a smaller lanthanide ionic radius, hardly form a glass and devitrify to orthoborate (LnBO_3) during quenching.⁴

As shown in Fig. 3, there is no spectral difference between the present lanthanide borate glasses, except for the small shift that is ascribed to the difference of the field strength of Ln^{3+} ions, as stated before. However, to investigate the structural units in the present glass systems quantitatively, using IR spectroscopy only is not considered to be sufficient. Here, we closely examine the borate network structure on the basis of Raman spectroscopy.

In Fig. 4, the Raman spectra of LaB_3O_6 metaborate crystal and $\text{La}_2\text{O}_3\text{-B}_2\text{O}_3$ glasses are shown. For 20 and 25 mol% of La_2O_3 , a well-developed Raman band appears at $\sim 770 \text{ cm}^{-1}$. Although this band is usually assigned to tetraborate groups, they should not be present at these compositions for $\text{La}_2\text{O}_3\text{-B}_2\text{O}_3$ glasses. Here, we tentatively have assigned this mode to the symmetric breathing vibration of the ladder-type ring unit that consists of two BO_3 trigonal and two BO_4 tetrahedral units,

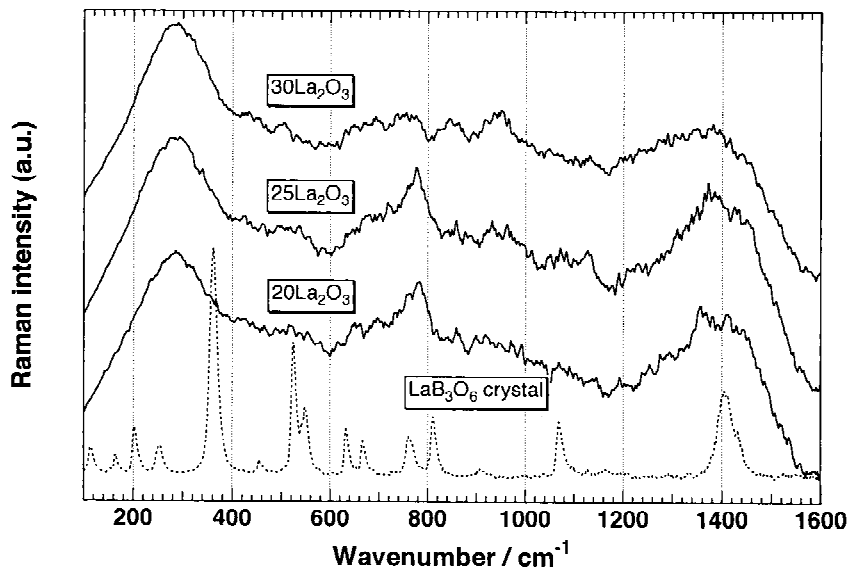


Fig. 4. Raman spectra of LaB_3O_6 crystal and $x\text{La}_2\text{O}_3 \cdot (100 - x)\text{B}_2\text{O}_3$ ($x = 20, 25,$ and 30) binary glasses.

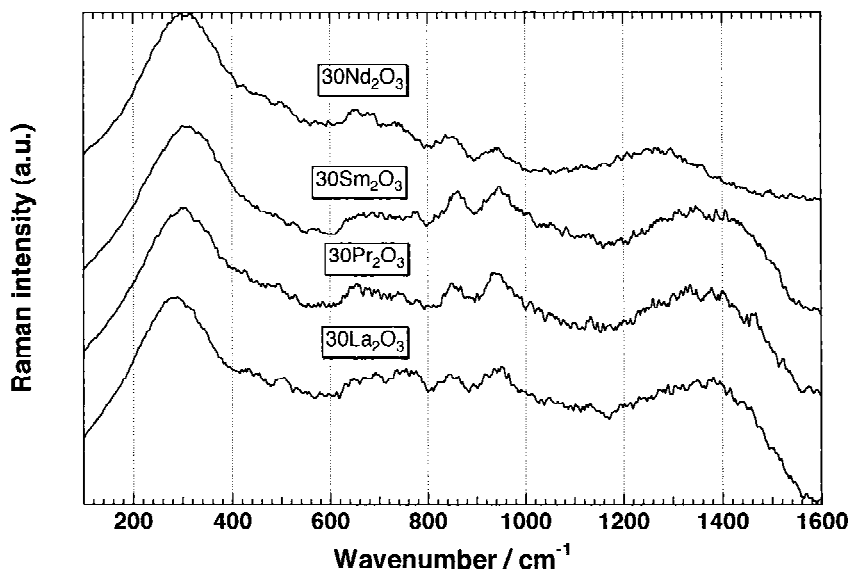


Fig. 5. Raman spectra of $30\text{Ln}_2\text{O}_3 \cdot 70\text{B}_2\text{O}_3$ ($\text{Ln} = \text{La}, \text{Pr}, \text{Nd},$ and Sm) binary glasses.

Table II. Assignments of Raman Spectra for Lanthanide Borate Glasses[†]

Wavenumber (cm ⁻¹)	Activity	Assignments
1250–1350	Medium	Stretching of BO_3 unit
920	Medium	Orthoborate group
820	Medium	Pyroborate group
770	Medium	Stretching of the ring unit
720	Medium	Diborate group
630–650	Medium	Metaborate groups
500	Weak	Isolated diborate group
300	Strong	Stretching of Ln–O bond

[†]Data from Meera and Ramakrishna.¹³

as is shown in Fig. 9. This assignment seems reasonable because the 770 cm^{-1} band is observed for the corresponding LaB_3O_6 crystal and the intensity is strongest at 25 mol% La_2O_3 . At 30 mol% of La_2O_3 , this broad band decreases drastically and new bands appear at 840 and 940 cm^{-1} , which are assigned to the pyroborate and orthoborate groups, respec-

tively. The Raman modes of $25\text{La}_2\text{O}_3 \cdot 75\text{B}_2\text{O}_3$ glass, as Chakraborty *et al.*³ stated, can be assigned based on its crystalline counterpart LaB_3O_6 ; this suggests that a basic similarity exists between the structures of $25\text{La}_2\text{O}_3 \cdot 75\text{B}_2\text{O}_3$ glass and its crystalline counterpart.

As shown in Fig. 4, for $30\text{Ln}_2\text{O}_3 \cdot 70\text{B}_2\text{O}_3$ glasses, the Raman bands are observed at $630\text{--}650\text{ cm}^{-1}$, which are assigned to the chain-type metaborate groups. Other bands, due to orthoborate, pyroborate, and diborate groups, indicate that these borate groups also are the structural units in these glasses. On the basis of these spectra, it is confirmed that the network structural units of $30\text{Ln}_2\text{O}_3 \cdot 70\text{B}_2\text{O}_3$ glasses are basically similar to each other.

(2) Linear and Nonlinear Optical Properties

Because the structural units of lanthanide borate glasses are basically similar to each other, it is considered that the $\chi^{(3)}$ values of these glasses elementally reflect the nonlinearity of rare-earth cations. Thus far, for the nonlinearity of lanthanide germanate glasses, Nasu *et al.*¹⁵ have concluded that it is the field strength of rare-earth cations that predominantly affects

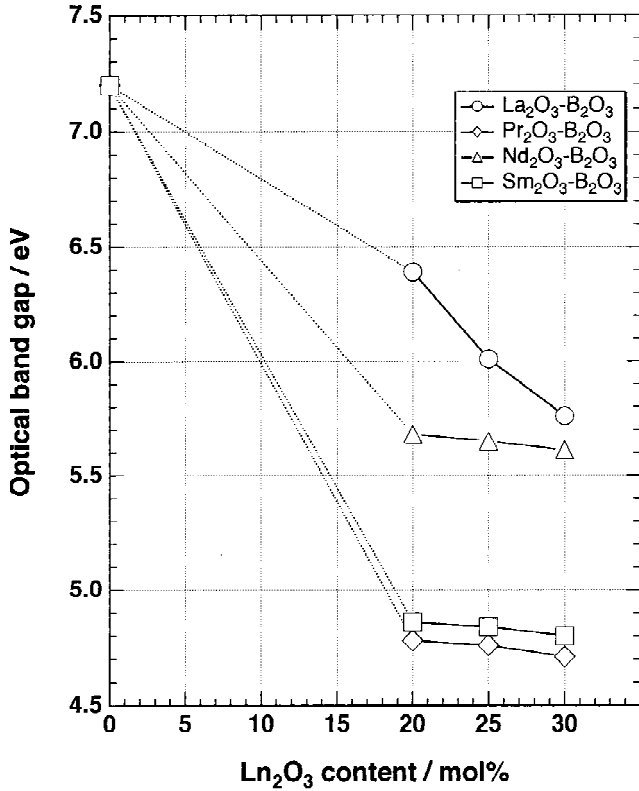


Fig. 6. Optical band gap (E_g) as a function of Ln_2O_3 content for $\text{Ln}_2\text{O}_3\text{-B}_2\text{O}_3$ ($\text{Ln} = \text{La}, \text{Pr}, \text{Nd}, \text{and Sm}$) binary glasses.

the nonlinearity; i.e., the weak-field-strength ions bind the valence electrons less tightly, which results in the large optical nonlinearity. As a consequence, lanthanum-containing glasses should have the largest $\chi^{(3)}$ values. However, such a simple model that neglects the contribution of the f - f electron transition cannot explain the nonlinearity of rare-earth cations sufficiently, as is evidenced in the present study. In this section, we discuss the optical nonlinearity in terms of the f - f electron transition and the optical band gap E_g .

As shown in Fig. 8, as the rare-earth content increases, E_g decreases in the following order of lanthanide elements: $\text{La} > \text{Nd} > \text{Sm} > \text{Pr}$. Because f orbitals have the same parity, the electronic dipole transition between $4f$ orbitals is forbidden, in principle. However, in the distorted ligand field, the f - f electron transitions are partly allowed and the oscillator strength has a value of 10^{-6} – 10^{-5} , which is much greater than that of the electronic quadrupole transition ($\ll 10^{-6}$). The absorption peaks in the visible region for praseodymium, neodymium, and samarium borate glasses are due to the electron transition between $4f$ orbitals. Meanwhile, for lanthanum borate glasses, there are no f electrons that contribute to the electron transition and no absorption bands in the visible region. Therefore, the NLO phenomena for lanthanum borate glasses are classified as “nonresonant-type” and the $\chi^{(3)}$ values of this system should not be so large.

On the other hand, praseodymium, neodymium, and samarium borate glasses have some absorption bands near the one-photon ($\sim 1.9 \mu\text{m}$), two-photon ($\sim 950 \text{ nm}$), and/or three-photon ($\sim 633 \text{ nm}$) excitations, because of the f - f electron transition, as shown in Fig. 1; therefore, these are classified as “resonant-type” glasses. It is considered that a virtual transition between $4f$ orbitals, as well as a transition between the valence band ($\text{O } 2p$) and the conduction band ($\text{Ln } 5d$), may contribute to the $\chi^{(3)}$ value of these glasses. In this case, a charge-transfer moment to the highest virtual states is induced, because of the presence of the real excitation states. In fact, the $\chi^{(3)}$ values of these resonant-type glasses are greater than that of lanthanum borate glasses, as shown in Fig. 8.

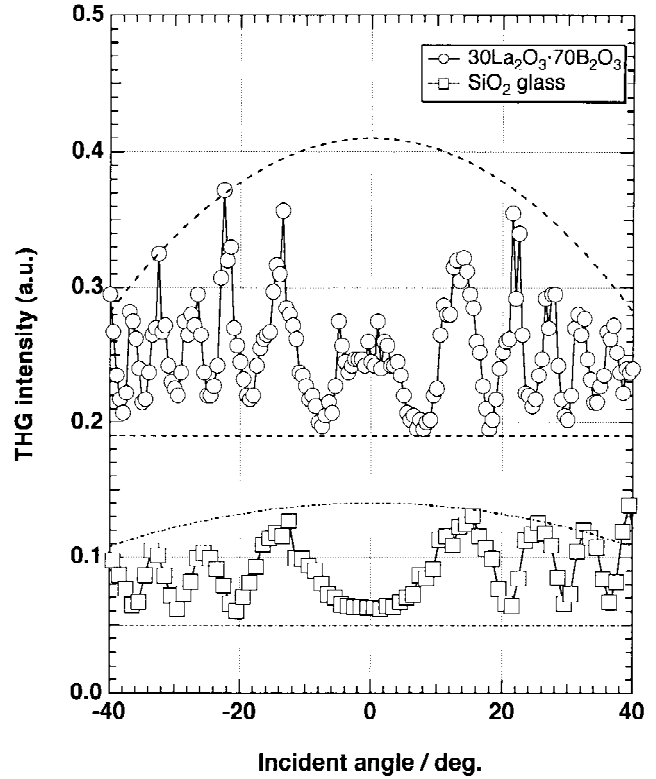


Fig. 7. Third harmonic intensity as a function of incident angle for (○) $30\text{La}_2\text{O}_3\cdot 70\text{B}_2\text{O}_3$ glass and (□) the reference SiO_2 glass.

Comparing neodymium and samarium borate glasses, the latter glasses have the larger $\chi^{(3)}$ values. This result may be interpreted by the optical resonance enhancement.^{9,16}

The quantum mechanical formula for cubic susceptibility that is responsible for the THG process is given by the following expression:¹⁷

$$\chi^{(3)} \propto \sum_{gmnm'} \Omega_{gn} \Omega_{nm} \Omega_{mn'} \Omega_{n'g} \times \left[\frac{1}{(E_{ng} - 3\omega)(E_{mg} - 2\omega)(E_{n'g} - \omega)} + \frac{1}{(E_{ng} + \omega)(E_{mg} - 2\omega)(E_{n'g} - \omega)} + \frac{1}{(E_{ng} + \omega)(E_{mg} + 2\omega)(E_{n'g} - \omega)} + \frac{1}{(E_{ng} + \omega)(E_{mg} + 2\omega)(E_{n'g} + 3\omega)} \right] \quad (3)$$

where E_{ij} is the energy difference between the j and i states in $h/(2\pi)$ units and Ω_{ij} are the transition matrix elements; the subscript g denotes the ground state and the subscripts n , m , and n' denote the excited states. When the third harmonic frequency (3ω) is close to the first allowed energy level (E_g), the dominant term in Eq. (3) should be the first one. Assuming that a third-order optical transition occurs between two levels and the optical-transition moment for the multiple excitation is constant, then $\chi^{(3)}$ is expressed by the following equation:¹⁸

$$\chi^{(3)} = \frac{\Phi}{(E_g - 3\omega)(E_g - 2\omega)(E_g - \omega)} \quad (3')$$

where Φ is a phenomenological parameter. In Fig. 10, $\chi^{(3)}$ is plotted as a function of the optical band gap E_g . The solid line

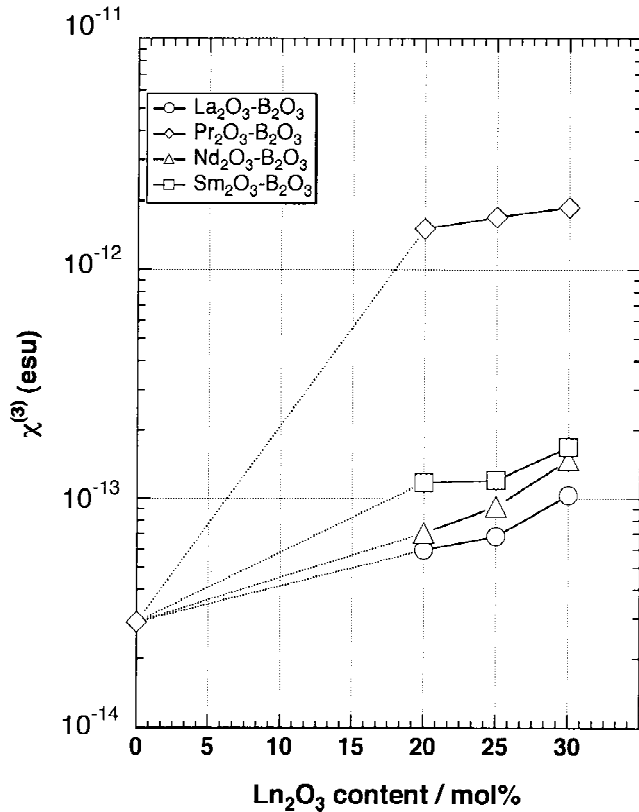


Fig. 8. $\chi^{(3)}$ as a function of Ln_2O_3 content for $\text{Ln}_2\text{O}_3\text{-B}_2\text{O}_3$ (Ln = La, Pr, Nd, and Sm) binary glasses.

that is shown in this figure represents the $\chi^{(3)}$ value that is predicted by Eq. (3'). The value of $\chi^{(3)}$ gradually increases as E_g decreases, which indicates that E_g is the dominant factor for the $\chi^{(3)}$ value of the lanthanide borate glasses, except for praseodymium borate glasses. As shown in this figure, E_g decreases in the following order of lanthanide elements: La > Nd > Sm. Such a reduction of E_g is the main reason for the larger $\chi^{(3)}$ values of samarium borate glasses.

On the other hand, praseodymium borate glasses have a $\chi^{(3)}$ value that is an order of magnitude greater than that of neodymium and samarium borate glasses. There may possibly be a contribution from the optical resonance enhancement, because of the smaller band gap. However, the wide deviation from the solid line, as shown in Fig. 10, suggests that there may be other mechanisms.

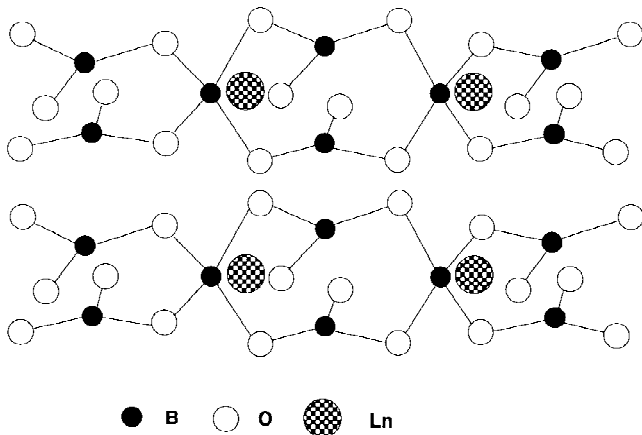


Fig. 9. Schematic structure model of lanthanide metaborate crystals (cited from Pakhomov *et al.*¹⁴).

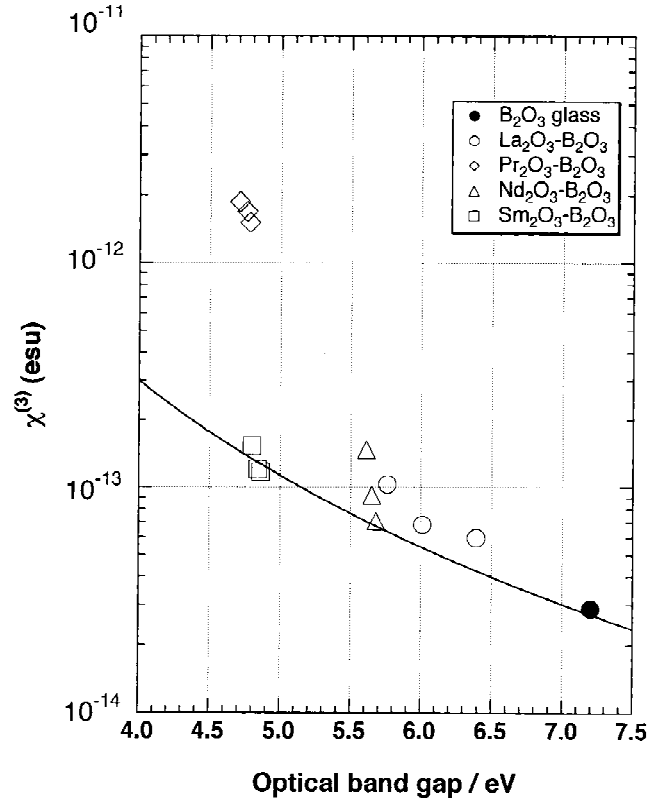


Fig. 10. $\chi^{(3)}$ as a function of the optical band gap (E_g) for $\text{Ln}_2\text{O}_3\text{-B}_2\text{O}_3$ (Ln = La, Pr, Nd, and Sm) binary glasses; the solid line is the fitting curve based on Eq. (3').

For praseodymium borate glasses, the one-photon energy certainly adjusts to one of the electronic states, as shown in Fig. 1. Accordingly, the $\chi^{(3)}$ values are enhanced drastically, because of the large transition moment to the first excitation state ($\Omega_{n'g}$). We have classified such an enhancement of nonlinearity as the "rigorous resonance effect."¹⁹ Despite the optical loss from the excited states, the $\chi^{(3)}$ value is, overall, quite large.¹⁹

The third-order optical nonlinearities are generally based on the trade-off between $\chi^{(3)}$ and optical absorption. Praseodymium borate glasses show high optical nonlinearity, in comparison with other lanthanide glasses, because of one-photon optical absorption. In addition to the practical application, this phenomenon is scientifically very interesting. Finally, further enhancement of $\chi^{(3)}$ might be accomplished by the simultaneous contribution from the Pr^{3+} ion and heavy-metal oxide ions such as Pb^{2+} and Bi^{3+} , which have a large polarizability.²⁰ A study of this system is now underway in our laboratory.

V. Conclusion

The third-order nonlinear susceptibility, $\chi^{(3)}$, of $\text{Ln}_2\text{O}_3\text{-B}_2\text{O}_3$ (Ln = La, Pr, Nd, and Sm) binary glasses was estimated by the third harmonic generation (THG) method. The glass structure also was investigated, based on IR and Raman spectroscopies. The following conclusions were obtained:

(1) It was reconfirmed that the network structures of lanthanide glasses with metaborate composition are similar to their crystalline counterpart (LnB_3O_6). The network structures of $\text{Ln}_2\text{O}_3\text{-B}_2\text{O}_3$ glasses were basically similar to each other.

(2) The $\chi^{(3)}$ values of praseodymium, neodymium, and samarium borate glasses were larger than lanthanum borate glasses, because of the optical resonance effect, in accordance with the $f\text{-}f$ electron transition.

(3) For praseodymium borate glasses, the $\chi^{(3)}$ value was enhanced considerably, because of the large transition moment to the first excitation state.

References

- ¹M. J. Weber, D. Milam, and W. L. Smith, "Nonlinear Refractive Index of Glasses and Crystals," *Opt. Eng.*, **17** [5] 463–69 (1978).
- ²E. M. Vogel, "Glasses as Nonlinear Photonic Materials," *J. Am. Ceram. Soc.*, **72** [5] 719–24 (1989).
- ³I. N. Chakraborty, J. E. Shelby, and R. A. Condrate, "Properties and Structure of Lanthanum Borate Glasses," *J. Am. Ceram. Soc.*, **67** [12] 782–85 (1984).
- ⁴I. N. Chakraborty, D. E. Day, J. C. Lapp, and J. E. Shelby, "Structure–Property Relations in Lanthanide Borate Glasses," *J. Am. Ceram. Soc.*, **68** [7] 368–71 (1985).
- ⁵I. N. Chakraborty and D. E. Day, "Effect of R^{3+} Ions on the Structure and Properties of Lanthanum Borate Glasses," *J. Am. Ceram. Soc.*, **68** [12] 641–45 (1985).
- ⁶T. Yongxing, J. Zhongong, and S. Xiuyu, "NMR, IR and Raman Spectra Study of the Structure of Borate and Borosilicate Glasses," *J. Non-Cryst. Solids*, **112**, 131–35 (1989).
- ⁷J. W. M. Verwey, G. F. Imbusch, and G. Blasse, "Laser Excited Spectroscopy of Gd^{3+} Ions in Crystalline and Glass Borate Hosts Comparable Composition," *J. Phys. Chem. Solids*, **50** [8] 813–20 (1989).
- ⁸E. V. Kolobkova, "Coordination States of Niobium and Its Structural Role in Lanthanum Borate Glasses According to Data from Vibrational Spectroscopy," *Fiz. Khim. Stekla*, **14** [4] 490–93 (1988).
- ⁹K. Terashima, S. H. Kim, and T. Yoko, "Nonlinear Optical Properties of B_2O_3 -Based Glasses: M_2O - B_2O_3 ($M = Li, Na, K, Rb, Cs, \text{ and } Ag$) Binary Borate Glasses," *J. Am. Ceram. Soc.*, **78** [6] 1601–605 (1995).
- ¹⁰K. Terashima, T. Hashimoto, and T. Yoko, "Nonlinear Optical Properties of B_2O_3 -Based Glasses: Binary Ag_2O - B_2O_3 and Ternary AgX - Ag_2O - B_2O_3 ($X = Cl, Br \text{ and } I$) Borate Glasses," *Phys. Chem. Glasses*, **37** [4] 129–33 (1996).
- ¹¹S. H. Wemple, "Refractive-Index Behavior of Amorphous Semiconductors and Glasses," *Phys. Rev. B: Solid State*, **7** [8] 3767–77 (1973).
- ¹²J. Krogh-Moe, "Interpretation of the Infra-Red Spectra of Boron Oxide and Alkali Borate Glasses," *Phys. Chem. Glasses*, **6** [2] 46–54 (1965).
- ¹³B. N. Meera and J. Ramakrishna, "Raman Spectral Studies of Borate Glasses," *J. Non-Cryst. Solids*, **159**, 1–21 (1993).
- ¹⁴V. I. Pakhomov, G. I. Sil'nitskaya, A. V. Medvedev, and B. F. Dzhurinskii, "Crystal Structure of Neodymium Metaborates," *Neorg. Mater.*, **8** [7] 1107–10 (1972).
- ¹⁵H. Nasu, J. Matsuoka, O. Sugimoto, M. Kida, and K. Kamiya, "Non-Resonant Type Third-Order Optical Nonlinearity of Rare Earth Oxides-Containing GeO_2 Glasses," *J. Ceram. Soc. Jpn.*, **101** [1] 43–47 (1993).
- ¹⁶N. F. Borrelli, B. G. Aitken, and M. A. Newhouse, "Resonant and Non-Resonant Effects in Photonic Glass," *J. Non-Cryst. Solids*, **185**, 109–22 (1995).
- ¹⁷F. Kajzar, J. Messier, and C. Rosilio, "Nonlinear Properties of Thin Films of Polysilane," *J. Appl. Phys.*, **60** [9] 3040–44 (1986).
- ¹⁸T. Hashimoto and T. Yoko, "Third-Order Nonlinear Optical Properties of Sol-Gel-Derived V_2O_5 , Nb_2O_5 , and Ta_2O_5 Thin Films," *Appl. Opt.*, **34** [16] 2941–48 (1995).
- ¹⁹Q. L. Zhou, J. R. Heflin, K. Y. Wong, O. Zamani-Khamiri, and A. F. Garito, "Enhanced Nonresonant Nonlinear Optical Processes from Populated Electronic Excited States," *Phys. Rev. A: Gen. Phys.*, **43** [3] 1673–76 (1991).
- ²⁰K. Terashima, T. Hashimoto, and T. Yoko, "Structure and Nonlinear Optical Properties of PbO - Bi_2O_3 - B_2O_3 Glasses," *Phys. Chem. Glasses*, **38** [4] 211–17 (1997). □